JOURNAL OF MATERIAL SCIENCE 33 (1998) 3151–3162

Adhesion and surface analysis of carbon fibres electrochemically oxidized in aqueous potassium nitrate

S. F. WASEEM, S. D. GARDNER*, GUOREN HE, WENBO JIANG‡, U. PITTMAN JR*‡
Department of Chemical Engineering, and ‡Department of Chemistry, Mississippi State University, Mississippi State, MS 39762, USA
E-mail: gardner@che.msstate.edu

Type II carbon fibres (PAN-based) have been electrochemically oxidized in aqueous potassium nitrate to varying electron charge densities (0–4294 C g^{-1}). The fibres were subsequently characterized by angle-resolved X-ray photoelectron spectroscopy (ARXPS) and ion scattering spectroscopy (ISS) and the results were correlated to acid/base surface titrations and BET surface area measurements. Relative to the as-received fibres (commercially treated, but unsized), the electrochemical treatments increased the ARXPS O/C atomic ratios by approximately 50%–100% and the concentration of oxidized carbon became more uniform within the XPS sampling depth ($\approx$ 10 nm). At the same time, the number of acidic functions titrated by sodium hydroxide rose from about 2.6 μeq g^{-1} to 1078 μeq g^{-1}, and the BET surface area increased from 0.67 $m^2 g^{-1}$ to 2.9 $m^2 g^{-1}$. A large portion of the increase in acidic groups was due to the increased fibre oxidation below the XPS sampling depth. The surface densities of acidic functions (functions/nm^2) determined from NaOH uptake and nitrogen BET surface area experiments were far larger than is physically possible. Thus, it is postulated that aqueous NaOH solutions are able to access a much larger surface region than can be measured by nitrogen BET. A model involving subsurface pores, voids, crevasses, etc., which become available via swelling during solvation in aqueous NaOH, but are at least partially closed off when dry (during BET measurements), was proposed. The quantity of acidic functions introduced (detected by NaOH) was directly proportional to the extent of oxidation as referenced to the electron charge density (C g^{-1}). The ISS spectra suggest that the surface density of carbon/oxygen groups was also increased. Single-fibre fragmentation tests (using an epoxy resin matrix) revealed that in most cases the interfacial shear strengths (IFSS) increased with increasing ARXPS O/C atomic ratio probably due to enhanced fibre/matrix chemical bonding and/or mechanical interlocking. As the extent of the electrochemical oxidation progressed above 1500 C g^{-1} the IFSS of single filament specimens then began to decrease. This was due to a continuing decrease in filament tensile strength as the extent of electro-oxidation increased. The critical transfer length, L_c, also decreased from $\sim$0.36 mm to $\sim$0.18 mm as the extent of electro-oxidation proceeded. Electrochemically oxidized fibres were compared to nitric acid-oxidized fibres in terms of acidic groups generated, BET surface areas, acidic group surface densities, dye adsorption with methylene blue and the role of aqueous NaOH in exposing some of the microstructure created by oxidative processes.

1. Introduction

The properties of composite materials are not only governed by the properties of the individual components, but also by the interface separating them [1–10]. Good interfacial bonding between composite constituents is necessary to couple their properties and enable adequate stress transfer. Because the interfacial properties depend to a large extent upon the surface composition and topography of the reinforcement, these parameters may be varied as a means to alter the effective properties of a given composite system.

Carbon fibres represent an important class of composite reinforcements due in part to their specific

*Authors to whom all correspondence should be addressed.

strength and stiffness [11]. These properties are derived from the graphitic microstructure of the fibres and the preferential alignment of graphitic crystallites along the fibre axis. Unfortunately, the adhesion characteristics of carbon fibres are often poor due to the high percentage of graphitic basal planes that comprise the surfaces. These basal planes are quite inert chemically, and so it is necessary to modify carbon fibre surfaces in order to enhance the adhesive properties.

Surface treatments may be beneficial to carbon fibre adhesion in several ways. By removing weak boundary layers and impurities, a more robust fibre surface is exposed [5, 8, 12, 13]. The fibre surface roughness may also be increased, promoting physical interlocking with the matrix [14–19]. Surface modification may also enhance the surface density of reactive functional groups. Depending upon the specific composite system, these functional groups may contribute to adhesion by enhancing the wetting characteristics of the fibres and/or creating the potential for chemical reaction with components in the matrix [4, 13–17, 20–27]. The latter case is particularly important with respect to carbon fibre-reinforced epoxy. Here, phenolic hydroxyl and carboxyl groups present on oxidized carbon fibre surfaces can react with epoxy functions and/or amine curing agents present in the matrix to form fibre-to-matrix covalent bonds.

The probability of chemically bonding certain polymers to carbon fibres will be proportional to the surface density of reactive groups on the fibres themselves. In the present investigation, carbon fibres have been functionalized via electrochemical treatment in potassium nitrate. The experiments are an extension of previous studies in which the central goal has been to maximize the extent of chemical bonding between carbon fibres and functions present in polyurethane prepolymers and epoxy resins [28–40]. The surface composition of the carbon fibres has been determined as a function of the electron charge density during treatment using angle-resolved X-ray photoelectron spectroscopy (ARXPS), ion scattering spectroscopy (ISS), and surface titration with aqueous sodium hydroxide. Single-fibre fragmentation experiments have also been performed in order to correlate further the data to the interfacial shear strengths of the resulting carbon fibre/epoxy specimens.

2. Experimental procedure

2.1. Materials

The carbon fibres used in this study were T-300, high-strength (Type II) fibres manufactured by Amoco Performance Products, Inc. The fibre roving contained about 3000 individual fibre filaments, each of which was approximately 7 μm in diameter. The as-received fibres were acquired without a sizing finish, and they had undergone a proprietary surface treatment by the manufacturer.

2.2. Carbon fibre surface treatments

The as-received fibres were electrochemically treated in aqueous potassium nitrate (Aldrich, ACS reagent grade) using a continuous process. Carbon fibres were pulled through a custom glass electrochemical cell in which the current through the electrolyte and the fibre residence time were both varied in order to achieve different electron charge densities. The fibres themselves served as the working electrode, whereas a stainless steel rod was the counter electrode. As shown in Table I, the as-received fibres were electrooxidized over a range of electron charge densities from 96–4112 C g^{-1}. At the exit region of the electrochemical cell, distilled water was allowed to run continuously over the fibre surfaces. Afterwards, the treated fibres were thoroughly rinsed with distilled water for a period of 2 d to remove residual electrolyte. The fibres were finally dried in ambient air at room temperature and stored in sterile polyethylene bags.

TABLE I The electrochemical oxidation parameters for each level of carbon fibre treatment

Specimen	[KNO_3] (wt %)	Current (A)	Residence time(s) [a]	Electron charge density (C g^{-1})
(a) as-received	–	–	–	–
(b)	2	0.6	46	96
(c)	1	0.08	748	112
(d)	1	0.4	804	602
(e)	2	0.5	1577	1475
(f)	2	0.6	1992	2237
(g)	2	0.6	3662	4112

[a] Electrochemical cell length was 140 cm for case (b), 259 cm for all others.

2.3. Carbon fibre surface titrations

Base uptake: the number of acidic functional groups present on the carbon fibres was determined by surface titrations using aqueous sodium hydroxide (Aldrich, ACS reagent grade). NaOH concentrations of 1×10^{-3} to 2×10^{-3} M were employed. Solutions were prepared from distilled water which was boiled before use to remove dissolved carbon dioxide. The carbon fibres (1 g) were immersed in sodium hydroxide and allowed to equilibrate for 10 h. Subsequently, the pH of the solution was measured (Ion Analyzer 250, Corning Industries) and compared with the solution pH value prior to fibre immersion. The net change in pH yielded the number of microequivalents of acidic functions present per gram of carbon fibre.

Methylene blue dye adsorption: methylene blue (MB^+) was selected as the dye for measuring acidic functions on carbon fibre surfaces. MB^+ solutions with a concentration of 20 mg l^{-1} (53.5×10^{-6} M) were employed. To adjust the pH to 10.8–11, 1 ml NaOH solution (1 M) was added to 1 l MB solution. At this pH the proton acid surface sites are deprotonated so that MB^+ can be taken up at these locations. Fibre specimens (1 g) were immersed in 50–300 ml MB^+ solution for 16 h. The volume used depended on the quantity of surface acidic functions present on the specimen as previously determined by base uptake. The absorbance of the remaining MB^+ solution was then meas-

ured by a spectrophotometer (Spectronic 21D, Milton Roy Co.) at 620 nm. Distilled water was used as a blank. The quantity of acidic functions determined by MB^+ adsorption was calculated from the change in dye concentration from before to after adsorption by the fibres.

2.4. Surface area measurements

The carbon fibre surface area was determined by nitrogen adsorption at $-196\,^{\circ}C$ according to the BET method (Quantasorb Surface Area Analyzer, Quantachrome Corporation). Fibre specimens (0.5–1.0 g) were outgassed at 250–300 °C in a mixture of helium (30 vol %) and nitrogen (70 vol %) for approximately 3 h prior to each measurement.

2.5. Surface characterization

Several 2.5 cm sections were cut from the carbon fibre rovings and positioned on top of a custom stainless steel sample holder. The fibres were held firmly in place by a gold foil mask secured to the sample holder with screws. The gold foil mask contained an oval machined in its centre that exposed a $1.5\,cm \times 0.8\,cm$ area of the underlying carbon fibres. The fibre specimen was positioned to ensure complete coverage of the stainless steel base below.

One fibre sample was analysed for each different surface treatment, but the physical dimensions of the fibres are such that photoelectrons (XPS) and ions (ISS) were collected from several tens of filaments during a single experiment. In this manner, there was multiple sampling with respect to the individual carbon fibre filaments. In order to render the data more representative of the fibres as a whole, the carbon fibre bundles comprising a given specimen were cut from different regions along the length of the fibre roving. Inasmuch as possible experimentally, the XPS and ISS data were acquired from a single location on each fibre specimen.

The X-ray photoelectron spectroscopy (XPS) and ion scattering spectroscopy (ISS) experiments were performed on a Physical Electronics Model 1600 surface analysis system. The instrument is based upon the Physical Electronics 10–360 spherical capacitor energy analyser (SCA) fitted with an Omni Focus III small-area lens (800 μm diameter analysis area) and high-performance multi-channel detection (MCD) technology. All of the data were acquired with the SCA operating in the fixed analyser transmission (FAT) mode. The XPS spectra were obtained using an achromatic MgK_α (1253.6 eV) X-ray source operated at 200 W. Survey scans were collected from 0–1100 eV with a pass energy equal to 46.95 eV, whereas high-resolution scans were performed over the ranges 0–110, 275–295, 390–410, 525–545 and 1055–1085 eV with the pass energy adjusted to 23.50 eV. Angle-resolved XPS (ARXPS) spectra were recorded after aligning the carbon fibres in the plane of the X-ray source and the SCA optics and subsequently tilting the specimen plane 10° and 90° with respect to the SCA entrance [6, 28–31]. ARXPS is now becoming a well-established technique for characterizing elemental depth profiles on oxidized carbon fibres [6, 28–31]. The surfaces of oxidized carbon fibres are typically rough, and (relative to a smooth surface) this somewhat decreases the level of surface sensitivity that can be obtained from ARXPS. However, theoretical considerations of XPS applied to several surface roughness profiles indicates that enhancement of surface sensitivity is frequently attainable through angle-resolving techniques [41, 42]. The time required to collect each set of ARXPS spectra at each electron take-off angle was approximately 3 h. Specimen surface degradation that might occur during the ARXPS experiments was assessed as outlined in previous studies [28–31] and found to be negligible. During all XPS experiments, the pressure inside the vacuum system was maintained at approximately 10^{-9} torr.

The ISS spectra were obtained using $^3He^+$ ions and a scattering angle of 135°. In order to maintain acceptable signal-to-noise and yet minimize sputter damage, the ion beam current density was adjusted to approximately 500 $nA\,cm^{-2}$ with a beam diameter of about 5 mm. The SCA pass energy used for ISS data acquisition was 187.85 eV. Typical data collection times were 1–2 min corresponding to a scattered ion energy ratio (E/E_0) ranging from 0.3–1.0. The system pressure was maintained near 10^{-7} torr (1 torr = 133.322 Pa) during the ISS experiments.

The XPS/ISS raw data were compiled and analysed using Physical Electronics Matlab (version 4.0) software. For calibration purposes, the carbon 1 s electron binding energy corresponding to graphite carbon was referenced at 284.6 eV [2]. Atomic ratios were calculated from the XPS spectra after background subtraction and correcting the relative peak areas by sensitivity factors based on the transmission characteristics of the Physical Electronics SCA [43].

2.6. Single filament tensile tests

The tensile strength of individual carbon fibres was measured according to ASTM D3379. Single-fibre filaments were bonded to paper tabs with an epoxy resin (Shell Epon 830 cured with TEPA). The specimen gauge lengths measured 12.7 mm and the testing speed was $0.52\,mm\,min^{-1}$. The breaking forces were measured using an electronic balance (Denver Instruments, model XL-1800) having an accuracy of 0.01 g. More than 100 fibre filaments were tested for each surface treatment. The breaking force data were fitted to a normal distribution function to obtain an average value. The tensile strength was calculated using the following relationship.

$$\sigma_f = \frac{4F}{\pi D^2} \tag{1}$$

where F is the breaking force and D is the filament diameter.

2.7. Single filament fragmentation tests

The interfacial adhesion between the fibre surfaces and an epoxy matrix was evaluated using single

filament fragmentation tests. Individual filaments of carbon fibre were positioned in the centre of dog-bone shaped specimens cast from Epon 830 epoxy resin (Shell Chemical Company). The epoxy was cured with TEPA tetraethylenepentamine in a weight ratio of 1 (Epon 830) : 0.21 (TEPA) for 4 h at 100 °C. The dog-bone specimens were subjected to an increasing tensile load until fibre breakage ceased to occur. The lengths of the fibre fragments were measured under a polarized light microscope (MicroMaster, model CK). Over 300 breaks per sample were employed to obtain the average fragment length for each extent of electro-oxidation. In some cases, from 600–1300 breaks were used but the values of L_c were found to be unchanged beyond 200–250 breaks. The number of single filament composites used for each determination was three to six in every case. The L_c values were fitted by a modified Weibull distribution function. The average length of the broken fibres represented the critical length, L_c. The interfacial shear strength, (τ), between the fibre surface and the epoxy matrix was calculated from Equation 2

$$\tau = \frac{D\sigma_f}{2L_c} \quad (2)$$

Where D is the filament diameter and σ_f is the filament tensile strength determined above.

3 Results and discussion

3.1 XPS experiments

In most cases, the XPS survey spectra (not shown) indicated that carbon and oxygen were the dominant species comprising the carbon fibre surfaces. The corresponding high-resolution C 1s and O 1s ARXPS spectra are shown in Fig. 1 for (a) the as-received carbon fibres and (b–g) fibres electrochemically oxidized in potassium nitrate in order of increasing electron charge density (see Table I). The solid and dashed curves represent XPS data collected at an electron take-off angle, α, equal to 10° and 90°, respectively. The average sampling depth is about 10–15 nm ($\alpha = 10°$) and 60–100 nm ($\alpha = 90°$). In order to facilitate comparisons, the spectra have been scaled with respect to the (arbitrary) intensity of the graphitic C 1s peak in Fig. 1a representing the as-received fibres. Inspection of Fig. 1a reveals it to be consistent with an as-received fibre that has already been oxidized to an appreciable extent. This is evident from the asymmetry of the C 1s peak towards higher binding energy relative to the graphitic reference peak at 284.6 eV. The peak asymmetry is due to various forms of oxidized carbon present as phenolic hydroxyl and/or ether groups (≈286.2 eV), carbonyl groups (≈287.6 eV), carboxyl and/or ester groups (≈288.8 eV) and/or possibly some carbonate groups near 290.6 eV [3, 43, 44]. The relative intensity of the O 1s peaks (Fig. 1a) is also suggestive of an oxidized carbon fibre surface. Consistent with the functional group assignments within the C 1s region above, these O 1s profiles may be deconvolved into two main peaks that correspond to C–O groups (≈531.5 eV) and

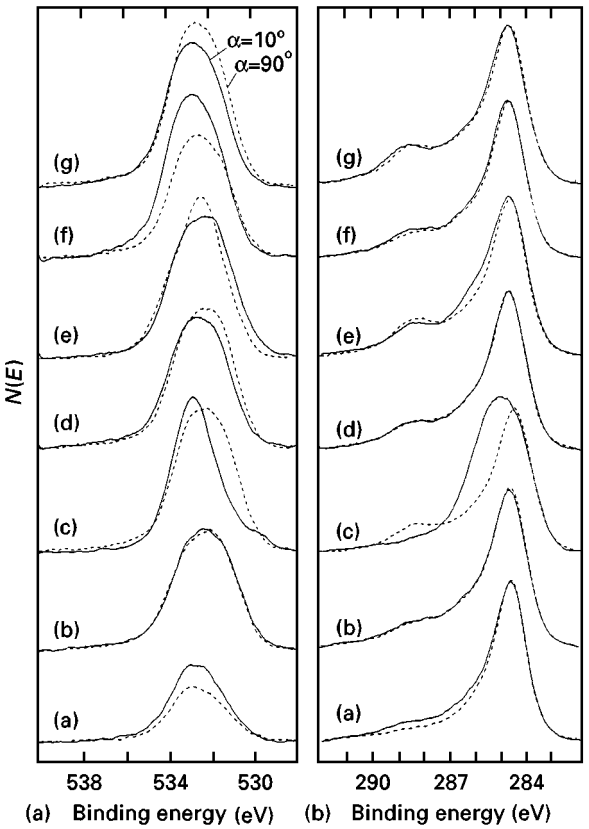

Figure 1 Angle-resolved XPS (ARXPS) (a) O 1s and (b) C 1s spectra acquired from (a) as-received carbon fibres, and fibres electrochemically oxidized in potassium nitrate at an electron charge density of (b) 96 C g^{-1}, (c) 112 C g^{-1}, (d) 602 C g^{-1}, (e) 1475 C g^{-1}, (f) 2237 C g^{-1} and 4112 C g^{-1}. Electron take-off angles: (—) 10° and (- - -) 90°.

C–OH and/or C–O–C groups (≈533 eV) [3, 44]. The relative intensities of the solid C 1s and O 1s spectra ($\alpha = 10°$) are greater than those of the dashed C 1s and O 1s spectra ($\alpha = 90°$) in Fig. 1a. This suggests that most of the oxidized carbon is located within the outermost 10–15 nm of the fibre surfaces which are more effectively probed at shallow electron take-off angles.

When the as-received carbon fibres are progressively exposed to an increasing electron charge density during the electrochemical oxidations, the ARXPS spectra in Fig. 1b–g indicates that the fibre surface composition changes considerably. The most obvious change is reflected in the increased O 1s/C 1s peak intensity ratio indicative of a more highly oxidized fibre surface. Considering the C 1s profiles, the main peak broadens toward higher binding energy and in most cases there is enhanced resolution of a feature near 288.6 eV. The former observation is consistent with an increased presence of hydroxyl groups, whereas the latter trend is consistent with an increase in the relative amount of carboxyl functions. Upon progressing through the series of treatments, the shapes of the C 1s spectra change in a manner that is consistent with a varying ratio of hydroxyl to carboxyl groups. For example, the hydroxyl/carboxyl group ratio appears greatest in the outermost layers (probed at ($\alpha = 10°$) of fibres oxidized with an electron charge density of 112 C g^{-1} (Fig. 1c). Here, there is a distinct increase in the (solid) C 1s peak intensity near 286 eV

and the carboxyl feature near 288.6 eV is barely visible. On the contrary, the relative presence of carboxyl groups is noticeably increased in Fig. 1g which corresponds to fibres exposed to an electron charge density of 4112 C g^{-1}. This overall behaviour is very similar to that observed by Jannakoudakis *et al.* [45]. They were able systematically to alter the relative presence of hydroxyl and carboxyl groups on PAN-based carbon fibres by varying the conditions of electrochemical oxidation.

The shapes of the C 1s profiles in Fig. 1 are also greatly influenced by the electron take-off angle, α. Therefore, the chemical composition of the carbon fibres is not uniform within the XPS sampling depth of approximately 0–10 nm. This is most obvious in Fig. 1c where hydroxyl groups (and/or ether functions) are the dominant form of oxidized carbon in the outermost fibre layers (solid spectrum, $\alpha = 10^{\circ}$). When the electron take-off angle is adjusted to 90° (dashed spectrum), the relative presence of hydroxyl/ether groups decreases with a concurrent increase in the relative concentration of carboxyl/ester functions. A similar trend is observed in Fig. 1e representing fibres oxidized with an electron charge density of 1475 C g^{-1}. These fibres had 424 μeq g^{-1} of acidic functions as measured by NaOH uptake. This emphasizes that substantial amounts of oxygen must reside in the concentric outer volume region of the fibres. In the case of Fig. 1b and 1d (electron charge densities of 96 and 602 C g^{-1}, respectively), the C 1s profiles nearly coincide, suggesting a uniform depth distribution of oxidized carbon has been achieved on these fibres. Based on these observations, it appears that the depth distribution of oxidized carbon does not follow a regular pattern with respect to the oxidation conditions investigated in this study.

The O 1s spectra in Fig. 1b–g generally reflect the behaviour observed in the corresponding C 1s profiles. The O 1s peak shape evolves through the series of fibre treatments consistent with changes in the type and relative presence of oxidized carbon groups. As expected, when hydroxyl and/or ether groups dominate the fibre surfaces (solid C 1s and O 1s spectra in Fig. 1c), there is a pronounced shift in the O 1s peak position to higher binding energy (≈533 eV). As the relative presence of carbonyl, carboxyl and/or ester groups increases, the O 1s peak width increases and there is a shift toward lower binding energy.

The ARXPS spectra in Fig. 1 clearly indicate that the number, identity and depth distribution of carbon/oxygen functions change during the electrochemical fibre treatments. Of particular interest is how the relative surface concentration of hydroxyl and carboxyl groups changes, because these species can undergo chemical reaction with a developing polyurethane interphase and/or epoxy matrix as discussed earlier. Features are easily resolved in Fig. 1 that are indicative of hydroxyl/ether and carboxyl/ester functions, but XPS is unable to provide a distinction within each group (i.e. hydroxyl versus ether and carboxyl versus ester) due to their overlapping binding energies. In order to provide additional information in this case, the carbon fibres have been titrated with

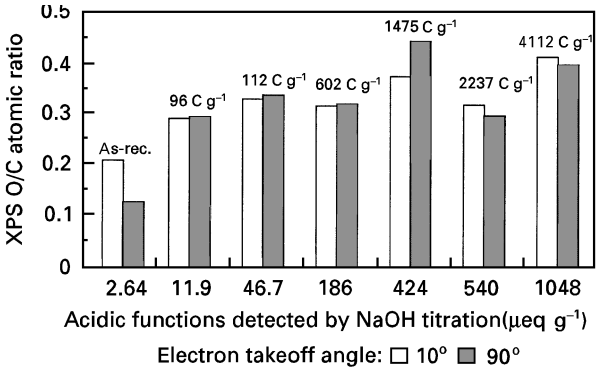

Figure 2 The relationship between the ARXPS O/C atomic ratios and the number of acidic functions on the fibre surfaces (measured by sodium hydroxide titration) at each level of fibre treatment investigated. The white and dark columns correspond to electron take-off angles of 10° and 90°, respectively. The numbers above the columns indicate the electron charge density for the six different fibre treatment levels (see Table I).

aqueous sodium hydroxide before and after each of the electrochemical oxidations. These data are illustrated in Fig. 2 where the number of acidic groups (μeq g^{-1} fibre) has been plotted against the ARXPS O/C atomic ratio for electron take-off angles of 10° and 90°. The corresponding electron charge densities (C g^{-1}) chosen for each fibre treatment appear above each column of data. As discussed below, the trends in Fig. 2 raise interesting questions about how fibre oxidation is progressing on these surfaces.

Approximately 2.64 μeq g^{-1} acidic groups (i.e. hydroxyl and/or carboxyl groups) are detected on the as-received fibres where the corresponding ARXPS O/C atomic ratios are 0.21 ($\alpha = 10^{\circ}$) and 0.13 ($\alpha = 90^{\circ}$). After one of the mildest electrochemical treatments (96 C g^{-1} charge density), the number of acidic groups detected increases to 11.9 μeq g^{-1}. At this point, the O/C atomic ratios recorded at both electron take-off angles have increased and nearly coincide at about 0.29. This suggests that the oxidation process is beginning to penetrate the outermost fibre layers deeper within the XPS sampling depth. Increasing the electron charge density beyond 96 C g^{-1} to 4112 C g^{-1} does ultimately increase the ARXPS O/C atomic ratio to near 0.40, but there is no direct correlation with the extent of oxidation. Over this same range of electron charge density, however, there is an enormous increase (from 11.9 μeq g^{-1} to 1048 μeq g^{-1}) in the number of acidic groups detected by sodium hydroxide titration. These results support the contention that the features in the ARXPS spectra of Fig. 1 are partially due to hydroxyl and carboxyl groups. However, the increase in acidic groups (two orders of magnitude) detected by surface titration is not reflected to nearly the same degree in the ARXPS data. The O/C ratios obtained by ARXPS do not even double over the range of electro–oxidation. There are two possible explanations for this behaviour based on the nature of each experiment. The surface titration experiments quantify an absolute number of acidic groups per gram of carbon fibre to a depth that is governed by the characteristic dimensions of the fibre porosity and microstructure. This may be contrasted

with the XPS experiment which measures the relative concentration of oxygen and carbon within a sampling depth of approximately 10 nm. An increase in the surface density of oxygen groups (i.e. groups per area of fibre surface) can only explain a small portion of the behaviour in Fig. 2, because the huge increase in the number of titratable acid groups (relative to the increase in the XPS O/C atomic ratio) is far too large to be entirely attributed to this occurrence. A more likely explanation might be an increase in the extent of fibre oxidation that has occurred beyond the XPS sampling depth with concurrent increase in the fibre surface area and microporosity. This would be consistent with previous investigations [11] where electrochemical oxidation of carbon fibres has altered both the surface composition and the fibre topography.

3.2. Surface area (BET) and NaOH uptake experiments

In order to assess the extent of topographical surface modification during the electrochemical treatments, the carbon fibres were subjected to BET surface area measurements and SEM. The scanning electron micrographs (not shown) did not exhibit visual evidence to indicate a change in the fibre topography as a function of the electrochemical treatments. The BET surface area of the as-received fibres was about $0.67\,m^2\,g^{-1}$. Progressing through the entire series of electrochemical treatments, the fibre surface area increased to approximately $2.9\,m^2\,g^{-1}$. The BET surface areas versus the extent of oxidation and amount of acidic groups present is given in Table II. The fourfold increase in fibre surface area is clearly insufficient to account for the overall increase in acidic groups detected by the surface titrations. As the extent of oxidation increases from 0 $C\,g^{-1}$ to 4112 $C\,g^{-1}$ the quantity of acid groups on the surface, detected by NaOH uptake, increased from 2.6 $\mu eq\,g^{-1}$ to 1048 $\mu eq\,g^{-1}$. A plot of the acidic functions (in $\mu eq\,g^{-1}$) generated on the fibre surfaces versus the extent of electrochemical oxidation is given in Fig. 3. The number of functions generated is directly proportional to the extent of oxidation. When the amounts of acidic groups are divided by the BET surface areas (for each level of oxidation) the density of acidic functional groups on the surface is given in $\mu eq\,m^{-2}$. These values range from $3.9\,\mu eq\,m^{-2}$ (as-received) to $500\,\mu eq\,m^{-2}$ (4112 $C\,g^{-1}$). Upon converting these values to acidic functions/nm^2 surface (see column 4 of Table II) the surface densities range from 2.4 functions/nm^2 (as-received) to 210 functions/nm^2 (1475 $C\,g^{-1}$) to 420 functions/nm^2 (4112 $C\,g^{-1}$). These functional group densities after progressive electrochemical oxidation are simply impossible to achieve physically. For example, if the entire surface consisted of lateral planes and if every surface carbon atom of these planes was oxidized to phenolic hydroxyl or carboxyl groups, then the maximum number of acidic groups per square nanometre which could be achieved is about 12–13! [46]. What model can possibly explain the factor of 32–35 times this maximum allowable density (12–13) that was observed after one of the most extensive fibre oxidation treatments (4112 $C\,g^{-1}$)? One is led to the conclusion that something must be occurring in the BET surface area measurements which greatly understates the "true surface" seen by aqueous NaOH solutions during the NaOH uptake experiments. Before introducing one possible explanation (model) a brief mention of some previous literature is in order.

The modest increase in fibre surface area which we observed via BET is typical of electrochemical oxidation [11, 12, 20, 47, 48]. In contrast, fibres oxidized in concentrated nitric acid can exhibit much greater surface areas (≈ 5–$50\,m^2\,g^{-1}$) which corresponds to ~ 25–$250\,\mu eq\,g^{-1}$ acidic groups if every surface atom was on a lateral plane and oxidized to an acidic group [11, 38, 46]. Typically, as HNO_3 oxidation proceeds to generate surface areas higher than 5–10 $m^2\,g^{-1}$ the surface density of acidic groups (functions/nm^2), as measured by NaOH uptake and BET adsorption, decreases even as the total amount of surface acidic groups goes up (see Table III, rows 5 and 6). For

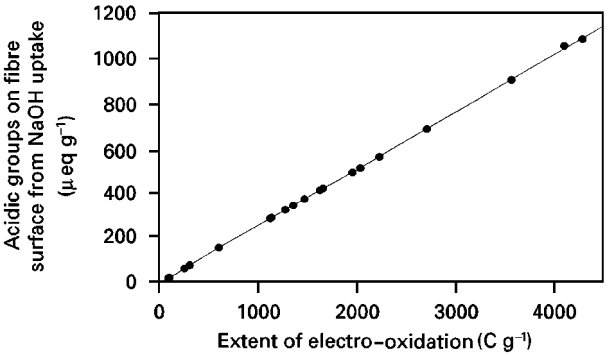

Figure 3 The introduction of acidic groups on carbon fibre surfaces versus the extent of electro-oxidation.

TABLE II Electrochemical oxidations of PAN-based T300 carbon fibres in aqueous KNO_3. Acidic functions, surface area and surface functional group densities versus the extent of oxidation

Extent of oxidation ($C\,g^{-1}$)	Acidic groups (NaOH uptake) ($\mu eq\,g^{-1}$)	Surface area N_2BET ($m^2\,g^{-1}$)	Apparent surface density of acidic groups (functions/nm^2)
0	2.6	0.67	2.4
96	11.9	0.84	
304	67	1.44	30
602	186	2.11	53
1126	258	1.81	
1360	338	4.41[a]	
1475	424	1.22	210
1664	433		
1962	551	1.38	241
2237	540		
2720	681	7.22[a]	
3581	898	2.17	
4112	1048	1.50	420
4294	1078	2.91	

[a] These samples employed a different steel electrode than the other experiments in this table. This steel electrode was thought to be stainless steel but it did show evidence of corrosion occurring when employed, unlike the other cases.

TABLE III The NaOH uptake, methylene blue (MB^+) adsorption, BET surface area, acidic functional group densities and ultraviolet adsorbances of aqueous NaOH washing solutions versus the length of T300 carbon fibre oxidations in 70 % HNO_3 at 115 % C

	Oxidation time (min)					
	0	20	40	60	90	105
NaOH uptake ($\mu eq\ g^{-1}$)	3.9	11.5	24.0	47.0	113	162
MB^+ adsorption ($\mu mol\ g^{-1}$)	1.98	3.38	4.31	4.63	22.03	37.2
Surface area based on MB^+ adsorption($m^2\ g^{-1}$)	2.36	4.03	5.14	5.52	26.3	44.4
Acidic function density based on the area calculated from MB^+ adsorption (Groups/nm^2)	1	1.7	2.8	5.12	2.6	2.2
Surface area based on N_2-BET ($m^2\ g^{-1}$)	0.65	0.73	1.65	2.09	12.4	18.8
Acidic function density based on BET area (Groups/nm^2)	3.6	9.5	8.8	13.5	5.5	5.2
UV (220 nm) absorbance of NaOH solutions after NaOH uptake experiment[a]	0.086	0.431	0.568	0.802	3.548	4.621

[a] The colour of NaOH solutions after being used for NaOH uptake became grey. The darker the colour, the higher was the solution absorbance at 220 nm. Oxidized fibres (1 g) were immersed into 30 ml 2×10^{-3} M aqueous NaOH in each experiment. The fibres were stirred gently for 10 h and then removed. The ultraviolet absorbance of these NaOH solutions was then taken immediately after the fibres were removed without any dilution.

example, for BASF (Celion G30-500) fibres (after 90 min oxidation in 70% HNO_3 at 115 °C) the surface area was $6.58\ m^2\ g^{-1}$ and $48.8\ \mu eq\ g^{-1}$ of acidic functions were found (by NaOH) on the surface [49]. This corresponds to 4.5 acidic groups/nm^2 ($\sim$35% of the theoretical maximum). Similarly Amoco (T300) fibres when oxidized identically for 90 min exhibited a BET surface area $12.4\ m^2\ g^{-1}$ and $113\ \mu eq\ g^{-1}$ of acid functions, corresponding to a surface density of 5.5 acidic functions per square nanometre ($\sim$45% of the maximum value) [50]. The situation is quite different for the electrochemically oxidized fibres where the apparent surface density of acidic groups continues to increase with oxidation time.

A situation similar to the present case of electrochemical oxidation has been documented for carbon fibres oxidized in Hummer's Reagent (a mixture of $NaNO_3$, H_2SO_4 and $KMnO_4$) where the number of acidic groups ranged from 200–835 $\mu eq\ g^{-1}$ and surface areas remained near $0.30\ m^2\ g^{-1}$ according to BET [11]. If this surface area is correct, one would expect $\sim 1.5\ \mu eq\ g^{-1}$ as the maximum amount of acidic groups possible (e.g. at 12.5 acidic functions per square nanometre).

A model is needed which can explain the large quantity of acidic groups which can be titrated by aqueous NaOH yet also accounts for the low BET surface areas measured (which are very low versus the surface area needed to hold all these acid groups). One approach is to conclude that nitrogen BET simply does not measure all the surface area which is accessible to aqueous NaOH. At first this seems impossible because a nitrogen molecule is smaller than a hydroxide ion and its water solvation shell. So nitrogen should be able to diffuse into any pores that aqueous NaOH could get into. However, if aqueous NaOH was able to swell a somewhat porous surface layer, then solvated hydroxide ions may be able to access a much larger surface area than would be exposed to nitrogen during BET measurements when the surface was dry. This model might be represented as a sponge. When dry and compressed only a limited fraction of the total internal surface area can be accessed because pathways (pores, holes, crevasses, etc.) to the interior (subsurface) are collapsed and closed off. A portion of the internal volume (and therefore the internal surface) is not present when the sponge is dry and collapsed. However, when the sponge is submerged in water it swells. The internal void volume (now full of water) has increased and the network of pores, holes and crevasses leading from the surface throughout the sponge is enlarged. Imagine the outer concentric graphitic layers of electrochemically oxidized carbon fibres being filled with cracks, pores, crevasses and internal voids which are interconnected to some depth below the surface (significantly below 1 nm, the depth probed by XPS). This internal morphology is created during the electrochemical oxidation when the fibre is submerged in aqueous electrolyte solutions. As oxidation proceeds, the oxidized regions become increasingly solvated (because keto, hydroxyl, carboxyl and other oxygenated groups are formed). This process promotes more oxidation in these regions because electrolyte gets into these regions and the electrochemical oxidation reactions occur at the graphite/solution interface. Furthermore, the fibres' original internal morphology has voids, flaws, crystal grain boundaries, etc., which differentially oxidize leading to the ultimate pattern of subsurface of oxidation microstructure and morphology of cracks, voids, pores, crevasses, etc.

After oxidation is completed, the fibres were thoroughly washed (removing electrolytes) and dried. During this process a portion of the internal volume and the pore/crack structure leading to it could close up as water evaporates. Thus, when a nitrogen BET measurement is made, a portion of the internal surface area which was present during oxidation is no longer accessible. Powerful solvation forces begin to act, however, when the fibres are submerged in aqueous

NaOH solutions. Aromatic hydroxyl and carboxyl groups are ionized to $-O^-Na^+$ and $-COO^-Na^+$ salt sites, respectively. These are exothermically solvated. The outer volume of the fibre containing the oxidized subsurface structures is swollen somewhat like a sponge taking up water. The opening of pathways to internal volume and the expansion of "collapsed" regions leads to a substantially greater surface (internal surface) becoming accessible to aqueous NaOH than had previously been available to nitrogen during the BET measurements. As a result of this process, the surface densities of acidic functions, obtained by dividing the number of these functions detected by NaOH by the BET surface area, is far too high. To obtain a "true" surface density (e.g. functions per square nanometre of graphite surface area), the surface area contacted by the aqueous NaOH solution would have to be known.

The model described above is, perhaps, somewhat exaggerated when using the sponge analogy. However, this generalized picture is clearly consistent with the oxidation of new surface area within the XPS sampling depth. This model would explain the increased XPS O/C atomic ratios in Fig. 2. If the surface density of oxygenated functions had also been increased, this too would remain consistent with the ARXPS trends. To remain consistent with the large number of acidic groups detected by the surface titration experiments, the surface density of acidic oxygenated functions must have been preferentially increased below the ARXPS sampling depth. The microstructure of PAN-based carbon fibres is characterized by highly convolved graphitic sheets that are preferentially aligned with the fibre axis. Numerous models of carbon fibres depict the microstructure as consisting of a surface region that is more graphitic, highly ordered and dense relative to the core region. The decreased ordering at some depth beneath the fibre surface would be expected to render this region more susceptible to chemical modification. In the present case, the fibre surface area has been increased by the electrochemical treatments, but the depth to which the new surface extends below the outer fibre periphery (as pores, crevasses, etc.) has not been determined. Based on Fig. 2, the oxidation appears to have influenced the fibre well beyond the outermost 1 nm. If the fibre subsurface (below the most highly crystalline surface region) consisted of a greater fraction of imperfections within the graphitic microstructure, then this region would be expected to contain a higher fraction of reactive sites prone to oxidation. Based on these considerations, an increase in the surface density of oxygen-containing functional groups (or O/C ratio) within this subsurface region might explain how the number of titrated acidic groups increased without a proportionate increase in the ARXPS O/C atomic ratio.

3.3. ISS experiments

Additional information about the carbon fibre surface composition is available from ISS. Because ISS probes the outermost layer only, it provides a direct measure of the surface density of carbon/oxygen functions that are not physically shadowed from the ion beam. Fig. 4 contains ISS spectra acquired from (a) the as-received carbon fibres and (b–g) fibres electrochemically treated in potassium nitrate in order of increasing electron charge density. All of the spectra have been scaled to a common (and arbitrary) oxygen peak intensity to facilitate comparisons. The ISS spectrum in Fig. 4a indicates that the outermost layer of the as-received fibre surface is essentially comprised of carbon and oxygen only. (Hydrogen will also be present, but ISS is not sensitive to hydrogen.) Fig. 4a is also consistent with the corresponding ARXPS spectra in Fig. 1a and the fact that the as-received fibres have been treated by the manufacturer to oxidize the surface. Fig. 4(b–g) indicate that the composition of the outermost atomic layer on these fibres changes as the charge density of the electrochemical treatments is increased. The O/C ratio increases on the outermost carbon layer upon oxidation. This trend indicates that the surface density of carbon/oxygen functional groups (i.e. number of groups per area of fibre surface) has indeed increased through the series of electrochemical treatments. This supports the hypothesis that the density of oxygenated functional groups is also increasing deeper beneath the fibre surface within features such as interconnected pores,

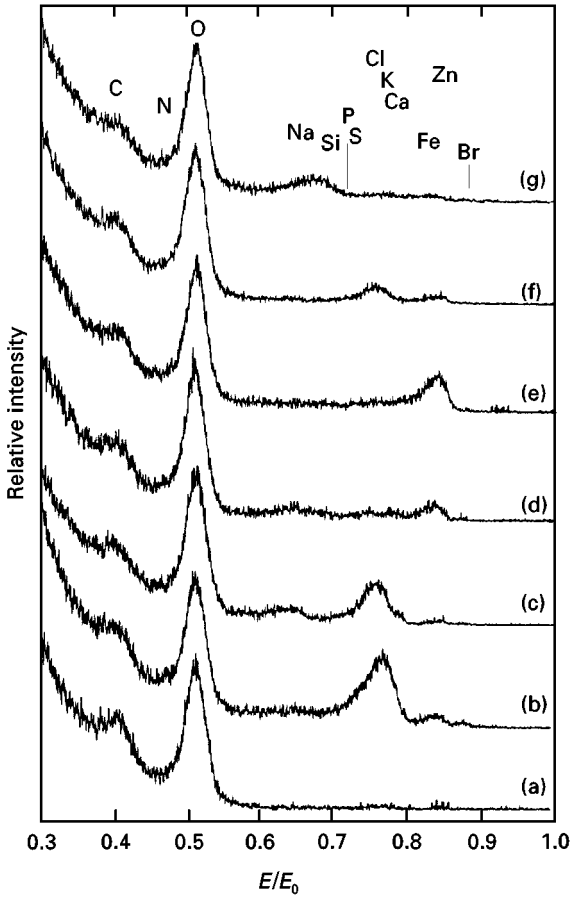

Figure 4 ISS spectra acquired from the (a) as-received carbon fibres, and fibres electrochemically oxidized in potassium nitrate at an electron charge density of (b) 96 $C\,g^{-1}$, (c) 112 $C\,g^{-1}$, (d) 602 $C\,g^{-1}$, (e) 1475 $C\,g^{-1}$, (f) 2237 $C\,g^{-1}$ and (g) 4112 $C\,g^{-1}$. The ISS peak positions for selected elements have been referenced at the top of the figure.

voids and crevasses that cannot be probed by ISS. Such features will constitute a substantial surface area located below the nominal outer fibre surface. Aqueous NaOH was able to penetrate into this microstructure and detect oxygenated acidic functional groups.

Fig. 4(b–g) also indicate that elements in addition to carbon and oxygen are present after the electrochemical treatments. In order to aid spectral interpretation, the ISS peak positions for several elements have been superimposed on top of Fig. 4. It is not implied that all of these elements are present. Of the elements shown, the presence of nitrogen, sodium, silicon, chlorine, calcium and iron was corroborated by the corresponding XPS survey spectra. Excepting nitrogen, the source of these additional elements is probably the environment within the electrochemical cell (i.e. the glass tubing, electrolyte solution and stainless steel electrode). Although nitrogen could have originated from the potassium nitrate electrolyte, the nitrogen concentration on these fibres did not vary significantly in either the ARXPS or ISS spectra. Nitrogen likely remains in the fibre due to incomplete conversion of the polyacrylonitrile (PAN) precursor. Inspection of Fig. 4 reveals that there is no clear trend with respect to the relative surface concentration of these additional elements. A very prominent feature due primarily to calcium ($E/E_0 \approx 0.78$) appears after the mildest electrochemical treatment (Fig. 4b, 96 C g^{-1}), but the intensity tends to moderate as the electron charge density is increased further. Potassium may also contribute to this feature; however, the presence of potassium was difficult to establish by XPS due to partial interference with the C1s features.

3.4. Comparison to carbon fibres oxidized in nitric acid

It is interesting to contrast these results with those from related investigations by the authors [29, 31]. In previous experiments, these same as-received carbon fibres have been oxidized in concentrated nitric acid for various times and temperatures. On average, ARXPS indicated that fibre oxidation in 70% nitric acid from 20–90 min at 115 °C increased the O/C atomic ratio to a level of about 0.25–0.30. The number of acidic groups measured by sodium hydroxide surface titrations increased from 12.5 μeq g^{-1} to 47.1 μeq g^{-1}. During this time, the surface density of carbon/oxygen functions as measured by ISS remained nearly constant. This suggested that the increased fibre oxidation must have occurred beneath the XPS sampling depth by the creation of additional surface area and its subsequent oxidation. This conclusion has since been supported further by BET experiments that indicate the fibre surface area increases from 0.67 m^2g^{-1} (as-received T300 fibres) to about 12.4 m^2g^{-1} (nitric acid exposure for 90 min at 115 °C) [46]. Several different studies of PAN-based carbon fibre oxidation in 70% HNO_3 (115 °C) in our laboratory have resulted in acidic functional group levels that range from 10–22 μeq g^{-1} after 20 min oxidation to 47–85 μeq g^{-1} after 90 min oxidation. The surface areas, measured by BET, after 90 min of oxidation have varied from 12–20 m^2g^{-1}. The systems with the highest level of acidic functions also had the higher surface areas.

Exposing nitric acid-oxidized fibres to aqueous sodium hydroxide has also been shown to remove oxidized graphitic fragments and some highly oxidized polynuclear aromatic materials from the partially oxidized surface layers. These substances were initially created by nitric acid treatment and their removal uncovered oxygen-rich regions that were previously beneath the XPS sampling depth [29]. Significantly, water washings were mostly clear and contained very little of this oxidized graphitic material which aqueous NaOH removed. Ionization of phenolic hydroxyl and carboxyl groups causes strong solvation forces to be manifest which, in turn help dislodge this material. These observations further support the concept that submerging oxidized fibres in an aqueous base can swell the surface region, exposing internal surface area (that was not available in the BET measurements).

The results of an example set of nitric acid oxidations of Thornel T300 (Amoco) carbon fibres are summarized in Table III. As-received fibres were oxidized for 20, 40, 60, 90 and 105 min in 70% HNO_3 at 115 °C. The quantity of acid functions on these fibres increased from 3.9 μeq g^{-1} (as-received) to 162 μeq g^{-1} (after 105 min oxidation). The surface areas determined by methylene blue (MB^+) adsorption increased from 23.6 m^2g^{-1} to 44.4 m^2g^{-1}. The increase in surface area was slow and steady through 60 min oxidation, followed by a rapid rise after 60 min. This same trend was seen in the nitrogen BET surface areas which ranged from 0.65 m^2g^{-1} (as-received) to 18.8 m^2g^{-1} (after 105 min oxidation). Again a rapid upturn in the rate surface area increase versus oxidation time occurs after 60 min nitric acid oxidation. The increase in surface area (BET) versus oxidation time is plotted in Fig. 5. The surface areas measured by MB^+ dye uptake are larger than those measured by nitrogen BET (Table III). Two factors probably combine to give this result. First, multilayer MB^+ adsorption probably occurs. Secondly, MB^+ is exposed to carbon fibre surfaces in aqueous base solutions which could increase the surface area available to the dye versus that available to nitrogen on dry fibre surfaces.

Table III also summarizes the absorbances of the (2×10^{-3} M) aqueous NaOH solutions which had been used in the NaOH uptake experiments. They became progressively darker with longer fibre oxidation times. These absorbance values are also plotted versus oxidation times in Fig. 5. Clearly, longer fibre oxidation times result in more oxidized aromatic and graphitic debris being removed from regions of the fibres at and near the surface upon exposure to aqueous NaOH.

In the present investigation, the electrochemical treatments have increased the ARXPS O/C atomic ratio on carbon fibres to levels comparable to those achieved using concentrated nitric acid as discussed above. Yet the number of acidic groups detected by sodium hydroxide surface titration is much larger for the electrochemically oxidized fibres. Given the results above for fibres oxidized in nitric acid, it is reasonable to conclude in the present case that a significant

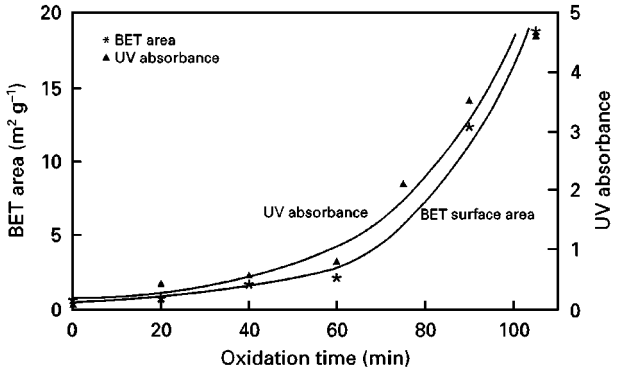

Figure 5 BET surface area and the ultraviolet absorbance of NaOH solutions after NaOH uptake by nitric acid-oxidized Thornel T300 carbon fibres versus oxidation time.

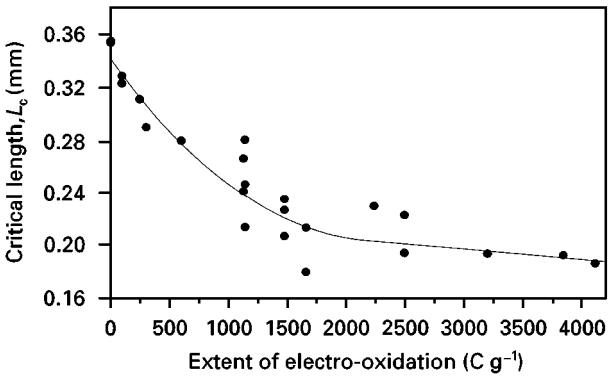

Figure 6 Critical transfer lengths L_c, from single filament fracture tests of T300 carbon fibres subjected to various extents of electro-oxidation in aqueous KNO_3.

amount of the increased oxidation has occurred beneath the XPS sampling depth. However, because the fibre BET surface area is less than that resulting from nitric acid oxidation, the surface density of carbon/oxygen groups must have been increased in order to compensate. This is consistent with the ISS spectra (outer atomic layer) in Fig. 4(b–g) where the oxygen/carbon peak intensity ratios are greater than those measured from fibres oxidized in nitric acid [29, 31].

3.5. Single filament fragmentation experiments

The interfacial shear strengths were calculated from single filament fragmentation testing. The critical transfer lengths, L_c, resulting from these tests are plotted versus the extent of electro-oxidation in Fig. 6. Electro-oxidation causes the values of L_c to decrease progressively with increasing electro-oxidation. The tensile strengths of the fibres versus oxidation extent were obtained from measurements of the breaking force for the filaments (Equation 1) as a function of the extent of electro-oxidation (shown in Fig. 7). From these determinations of σ_f and L_c the interfacial shear strengths, τ, were determined using Equation 2. A computer-smoothed plot of τ versus the extent of oxidation is also shown in Fig. 7. The interfacial shear strengths increase with oxidation up to oxidation levels of about 1500 C g^{-1}. Then the values of τ decrease due to progressive loss of fibre tensile strength, σ_f, as oxidation proceeds further.

Interfacial shear strengths appear in Fig. 8 representing (a) the as-received fibres and (b–g) fibres electrochemically oxidized in order of increasing electron charge density up to 4112 C g^{-1}. The data have been correlated to the ARXPS O/C atomic ratios measured at $\alpha = 10°$(■) and $\alpha = 90°$(○); hence two data points appear for each value of the interfacial shear strength. Examining these data it is apparent that in most cases the interfacial shear strengths (IFSS) increase with increasing O/C atomic ratio. The most obvious exception is Fig. 4g which represents fibres subjected to the highest electron charge density (4112 C g^{-1}). These fibres exhibited the lowest IFSS of the group (see Fig. 8), yet the ARXPS O/C atomic ratios were among the highest of those measured. However, single filament tensile tests demonstrated this was a consequence of the degradation of filament tensile strength which greatly decreased the IFSS at such an advanced electro-oxidation treatment level. (During the electrochemical treatments there was continual reduction in the fibre tensile strength which was ultimately decreased by about 45%). This would be consistent with

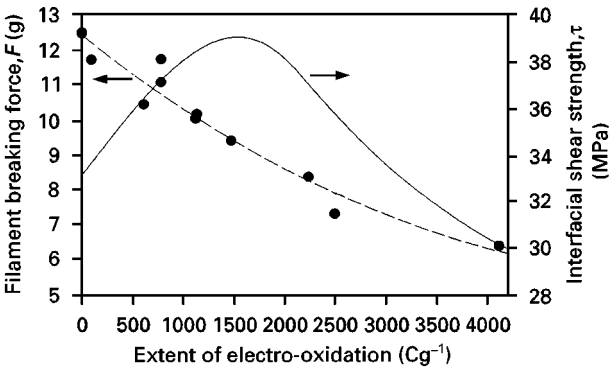

Figure 7 (–●–) Filament breaking forces (g) versus (—) the extent of electrochemical oxidation for carbon fibres used in single filament fracture tests.

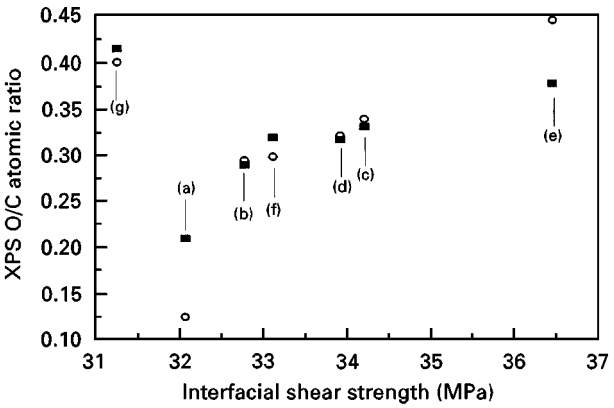

Figure 8 The interfacial shear strengths (measured by single-fibre fragmentation tests) of the carbon fibres measured in epoxy as a function of the ARXPS O/C atomic ratio of the fibres. The fibre surface treatments correspond to (a) as-received fibres, and fibres electrochemically oxidized in potassium nitrate at an electron charge density of (b) 96 C g^{-1}, (c) 112 C g^{-1}, (d) 602 C g^{-1}, (e) 1475 C g^{-1}, (f) 2237 C g^{-1} and (g) 4112 C g^{-1}. Electron take-off angles: (■) 10° and (○) 90°.

the previous hypothesis that these electrochemical oxidations progressively etch the fibres thereby increasing the surface area and the extent of microporosity below the outer fibre periphery. As the fibres are electrochemically oxidized, the increased surface roughness may promote better adhesion by providing for mechanical interlocking with the epoxy matrix. Furthermore, as the number of carboxyl and hydroxyl functions is increased on the fibres, the potential for fibre matrix chemical bonding is increased, and the fibre wetting characteristics would be improved to aid resin penetration into larger pores as described above. The behaviour in Fig. 8 would be expected if adhesion improvements due to these two mechanisms (mechanical interlocking and fibre matrix chemical bonding) were eventually offset by loss of fibre strength and overall fibre integrity. Furthermore, as the level of oxidation advances, the porosity increases. The size and number of crevasses, voids, etc., in the outer regions of the fibre are increased. Therefore, this region weakens. Thus, fibre–matrix interface failure may be replaced by failure of the outer carbon fibre layers. Apparently, the relative rates of these processes are such that higher surface treatment levels do not necessarily translate into enhanced adhesion as measured by the single fibre fragmentation test. This is consistent with results from similar investigations by Ballie and Bader [4] and Donnet and Guilpain [48].

4. Conclusion

The surface composition of type II, PAN-based carbon fibres (commercially treated, but unsized) has been investigated as a function of their exposure time to electrochemical treatment in potassium nitrate. The exposure times corresponded to six different electron charge densities ranging from 96–4112 $C\,g^{-1}$. Angle-resolved XPS (ARXPS) indicates that the O/C atomic ratios increased from about 0.20 (as-received fibres) to near 0.40 through the series of progressive electrochemical oxidations, and the oxidized carbon became more uniformly distributed within the XPS sampling depth ($\approx$10 nm) progressing inward (below the surface) with time. The ARXPS data were subsequently correlated to the number of surface acidic groups on the fibres (detected by titration with sodium hydroxide) and BET surface area measurements. As the electron charge density was increased, the number of acidic groups on the fibres increased from 2.64 μeq g^{-1} (as-received fibres) to approximately 1078 μeq g^{-1} (4294 $C\,g^{-1}$). This occurred while the BET surface area of the as-received fibres (0.67 m^2g^{-1}) did not increase beyond 2.9 m^2g^{-1} at very high levels of oxidation. This led to surface densities of 200–420 acidic groups per square nanometre of surface. Such functional group densities are physically impossible. The data were logically explained by a model in which aqueous NaOH can swell the outer concentric volume of the fibre through its network of cracks, pores, fissures and crevasses which are lined with oxygenated functional groups. Upon drying, this region collapses such that only a much smaller total surface area can be measured by nitrogen BET.

The large number of acidic groups detected by the titration experiments suggests that changes observed in the ARXPS C 1s and O 1s peak shapes were due largely to a changing ratio of hydroxyl groups/carboxyl groups on the fibre surfaces. This is noteworthy because hydroxyl and carboxyl groups can chemically react with functions present in an epoxy matrix and contribute towards improved adhesion. However, the proliferation of acidic functions was not proportionate to (but greater than) the increased XPS O/C atomic ratios, suggesting that additional oxidation of the fibres occurred below the XPS sampling depth. Given the relatively modest increase in the fibre surface area, it is hypothesized that the increased fibre oxidation is brought about primarily by an enhanced surface density of carbon/oxygen groups within pores and crevasses extending beyond 10 nm beneath the outer fibre periphery. This hypothesis is further supported by ISS spectra in which the O/C peak intensity ratio is increased during the series of fibre treatments.

The adhesion characteristics of the carbon fibres have also been examined using single-fibre fragmentation experiments. The data indicate that the fibre/epoxy interfacial shear strengths (IFSS) correlate well with the ARXPS O/C atomic ratios except at the highest level of fibre treatment investigated (4112 $C\,g^{-1}$) in these single fibre fracture tests. The data are consistent with enhanced adhesion due to fibre/matrix chemical bonding and/or mechanical interlocking. However, only a small fraction of all the acidic functions introduced, as oxidation proceeds, are available to bind to the epoxy matrix resin at the outer graphitic layer of the fibre. As the maximum level of electrochemical treatment is approached, the fibre strength is compromised to a point ultimately resulting in a net decrease in the IFSS.

Acknowledgements

This research was supported in part by the National Science Foundation through Grants STI-8902064, EHR-9108767 and EPS-9452857. Support from the State of Mississippi and Mississippi State University is also gratefully acknowledged. S. D. Gardner and C. U. Pittman Jr, acknowledge the National Science Foundation (Grant CTS-9212295), Mississippi State University and the Department of Chemical Engineering, for providing funds to purchase the XPS/ISS instrumentation.

References

1. C. A. BALLIE, J. E. WATTS, J. E. CASTLE and M. G. BADER, *Compos. Sci. Technol.* **48** (1993) 97.
2. T. WANG, P. M. A. SHERWOOD, *Chem. Mater.* **6** (1994) 788.
3. Y. XIE, and P. M. A. SHERWOOD, *ibid.* **2** (1990) 293.
4. C. A. BALLIE and M. G. BADER, *J. Mater. Sci.* **29** (1994) 3822.
5. C. JONES, *Surf. Interface Anal.* **20** (1993) 357.
6. *Idem*, *Compos. Sci. Technol.* **42** (1991) 275.
7. J. D. H. HUGHES, *ibid.* **41** (1991) 13.
8. L. T. DRZAL, in "Advances in Polymer Science", edited by K. Dusek, Vol. 75 (Springer, Berlin 1986) pp. 1–32.

9. H. ISHIDA (ed.), "Controlled Interphases in Composite Materials" (Elsevier, New York, 1990).
10. M. R. PIGGOTT, *Compos. Sci. Technol.* **42** (1991) 1.
11. J. B. DONNET and R. C. BANSAL, in "Carbon Fibers" (Marcel Dekker, New York, 1990) pp. 145.
12. F. NAKAO, Y. TAKENAKA and H. ASAI, *Composites* **23** (1992) 365.
13. L. T. DRZAL, M. J. RICH and P. F. LLOYD, *J. Adhes.* **16** (1982) 1.
14. J. HARVEY, C. KOZLOWSKI and P. M. A. SHERWOOD, *J. Mater. Sci.* **22** (1987) 1585.
15. B. Z. JANG, *Compos. Sci. Technol.* **44** (1992) 333.
16. R. YOSOMIYA, K. MORIMOTO, A. NAKAJIMA, Y. IKADA and T. SUZUKI (eds), in "Adhesion and bonding in composites" (Marcel Dekker, New York, 1990) pp. 257–80.
17. A. J. VUKOV, *J. Serb. Chem. Soc.* **55** (1990) 333.
18. P. W. YIP and S. S. LIN, *Mater. Res. Soc. Symp. Proc.* **170** (1990) 339.
19. M. GUIGON and E. KLINKLIN, *Composites* **25** (1994) 534.
20. E. FITZER and R. WEISS, *Carbon* **25** (1987) 455.
21. C. U. PITTMAN Jr, S. D. GARDNER, G. HE, L. WANG, Z. WU, C. SINGAMSETTY, B. WU and G. BOOTH in "Proceedings of the Spring 1995 Materials Research Society Meeting", Vol.383, Polymer/Inorganic Interfaces II. (Materials Research Society, Pittsburgh, PA) p. 195. Eds: L. T. Drzal, R. L. Opila, N. A. Peppas and C. Schutte. Published in 1995.
22. J. B. DONNET, E. PAPIRER and H. DAUKSCH, in "Carbon Fibers-Their Place in Modern Society" (The Plastics Institute, London, 1974) pp. 58.
23. E. FITZNER, and H. P. RENSCH, in "Controlled Interphases in Composite Materials", edited by H. Ishida (Elsevier, New York, 1990) pp. 241–54.
24. G. KREKEL, U. J. ZIELKE, K. J. HÜTTINGER, and W. P. HOFFMAN, *J. Mater. Sci.* **29** (1994) 3984.
25. K. J. HÜTTINGER, G. KREKEL and U. ZIELKE, *J. Appl. Polym. Sci.* **51** (1994) 737.
26. N. L. WEINBERG and T. B. REDDY, *J. Appl. Electrochem.* **3** (1973) 73.
27. B. W. CHUN, C. R. DAVIS, Q. HE and R. R. GUSTAFSON, *Carbon* **30** (1992) 177.
28. S. D. GARDNER, C. S. K. SINGAMSETTY, G. L. BOOTH, G. R. HE and C. U. PITTMAN Jr, *Carbon* **33** (1995) 587.
29. S. D. GARDNER, C. S. K. SINGAMSETTY, Z. WU and C. U. PITTMAN Jr, *Surf. Interface Anal.* **24** (1996) 311.
30. S. D. GARDNER, C. S. K. SINGAMSETTY, G. HE and C. U. PITTMAN Jr, *Appl. Spectros.* **51** (1997) 636.
31. E. D. PERAKSLIS, S. D. GARDNER and C. U. PITTMAN Jr, *J. Adhes. Sci. Technol.* **11** (1997) 531.
32. C. U. PITTMAN Jr, G. HE, B. WU, L. WANG and S. D. GARDNER, in "Extended abstract of the Fifth International Conference on Composite Interfaces", Göteborg, 20–23 June 1994, pp. 19–2.
33. C. U. PITTMAN Jr, G. HE, B. WU, L. WANG and S. D. GARDNER, in "Proceedings of the First International Conference on Composites Engineering", New Orleans, 28–31 August 1994, pp. 403. The International Community for Composite Engineering (ICCE) joint with the University of Neworleans.
34. S. D. GARDNER, C. S. K. SINGAMSETTY, E. D. PERKSLIS, Z. WU and C. U. PITTMAN Jr, in "Proceedings of the Second International Conference of Composites Engineering", New Orleans, 21–24 August 1995, pp. 583.
35. S. D. GARDNER, C. S. K. SINGAMSETTY, G. HE and C. U. PITTMAN Jr, *ibid*., pp. 677. The International Community for Composite Engineering (ICCE) joint with the University of Neworleans.
36. S. D. GARDNER, E. D. PERAKSLIS and C. U. PITTMAN Jr, in "Proceedings of the Third International Conference on Composites Engineering", New Orleans, 21–26 July 1996, pp. 293. The International Community for Composite Engineering (ICCE) joint with the University of Neworleans.
37. S. D. GARDNER, G. HE, W. JIANG and C. U. PITTMAN Jr, *ibid*., pp. 681. The International Community for Composite Engineering (ICCE) joint with the University of Neworleans.
38. Z. WU, C. U. PITTMAN Jr and S. D. GARDNER, *Carbon* **34** (1996) 59.
39. *Idem*, *ibid*. **33** (1995) 607.
40. *Idem*, *ibid*. **33** (1995) 597.
41. C. S. FADLEY, R. J. BAIRD, W. SICKHAUS, T. NOVAKOV and S. Å. L. BERGSTRÖM, *J. Electron Spectrosc. Rel. Phenom.* **4** (1974) 93.
42. R. J. BAIRD, C. S. FADLEY, S. K. KAWAMOTO, M. MEHTA, R. ALVAREZ and J. A. SILVA, *Analyt. Chem.* **48** (1976) 843.
43. J. F. MOULDER, W. F. STICKLE, P. E. SOBOL and K. D. BOMBEN, in "Handbook of X-ray Photoelectron Spectroscopy", edited by J. Chastain (Perkin-Elmer Corporation, Eden Prairie, MN, 1992) pp. 253.
44. G. BEAMSON and D. BRIGGS, in "High Resolution XPS of Organic Polymers. The Scienta ESCA300 Database" (Wiley, Chichester, 1992).
45. A. D. JANNAKOUDAKIS, P. D. JANNAKOUDAKIS, E. THEODORIDOU and J. O. BESENHARD, *J. Appl. Electrochem.* **20** (1990) 619.
46. G. HE, PhD dissertation, Mississippi State University (1994).
47. P. EHRBURGER and J. B. DONNET, *Phil. Trans. R. Soc. Lond. A* **294** (1980) 495.
48. J. B. DONNET and G. GUILPAIN, *Composites* **22** (1991) 59.
49. C. U. PITTMAN Jr, G. R. HE, B. H. WU and S. D. GARDNER, *Carbon* **35** (1997) 330.
50. C. U. PITTMAN Jr, Z. WU, W. JIANG, G. R. HE, B. H. WU. W. LI and S. D. GARDNER, *Carbon* **35** (1997) 929.

Received 11 December 1996
and accepted 18 March 1998